Integrated Ocean Drilling Program
Expedition 328 Scientific Prospectus

Cascadia Subduction Zone ACORK Observatory

Earl Davis
Pacific Geoscience Centre
Geological Survey of Canada
9860 W. Saanich Road
Sidney British Columbia V8L 4B2
Canada

Katerina Petronotis
Expedition Project Manager/Staff Scientist
Integrated Ocean Drilling Program
Texas A&M University
1000 Discovery Drive
College Station TX 77845-9547
USA

Kusali Gamage
Expedition Project Manager/Staff Scientist
Integrated Ocean Drilling Program
Texas A&M University
1000 Discovery Drive
College Station TX 77845-9547
USA

Publisher's notes

Material in this publication may be copied without restraint for library, abstract service, educational, or personal research purposes; however, this source should be appropriately acknowledged.

Distribution:
Electronic copies of this series may be obtained from the Integrated Ocean Drilling Program (IODP) Scientific Publications homepage on the World Wide Web at **www.iodp.org/scientific-publications/.**

Disclaimer

This IODP *Scientific Prospectus* is based on precruise Science Advisory Structure panel discussions and scientific input from the designated Co-Chief Scientists on behalf of the drilling proponents. During the course of the cruise, actual site operations may indicate to the Co-Chief Scientists, the Staff Scientist/ Expedition Project Manager, and the Operations Superintendent that it would be scientifically or operationally advantageous to amend the plan detailed in this prospectus. It should be understood that any proposed changes to the science deliverables outlined in the plan presented here are contingent upon the approval of the IODP-USIO Science Services, TAMU, Director in consultation with IODP-MI.

Abstract

Operations to be carried out during Integrated Ocean Drilling Program Expedition 328 will be devoted to the installation of a new permanent hydrologic observatory at Ocean Drilling Program (ODP) Site 889, the location originally chosen for a Circulation Obviation Retrofit Kit (CORK) installation during ODP Leg 146. During that attempt, rapid sediment intrusion into the perforations and bottom of an open-ended casing liner prevented proper sealing of the hole, and the objectives for the original CORK monitoring were never met. The format of the new installation will follow the Advanced CORK (ACORK) design, developed initially for installations at the Nankai subduction zone during ODP Leg 196. This configuration will facilitate pressure monitoring at multiple formation levels on the outside of a 10¾ inch casing string. The casing will be sealed at the bottom, leaving the inside available for future installation of additional monitoring instruments. Although drilling operations will be highly focused in a short period of time on site, a broad range of objectives will be addressed with monitoring over the decades to follow. These will include documenting the average state of pressure in the frontal part of the Cascadia accretionary prism, the pressure gradients driving flow from the consolidating sediments, the mode of formation of gas hydrates, the influence of hydrates and free gas on the mechanical properties of their host lithology, the response of the material to seismic ground motion, and the magnitude of strain at the site caused by episodic seismic and aseismic slip in this subduction setting. Initial instrumentation will include autonomously recorded seafloor and formation pressure sensors and seafloor temperature sensors. These, and other downhole instruments to measure temperature, tilt, and seismic ground motion to be deployed at a later date by submersible, will be connected to the NEPTUNE fiber-optic cable for power and real-time communications from land.

Background

Previous drilling at Site 889

Ocean Drilling Program (ODP) Leg 146 was devoted to documenting the evolution of turbidite sediments as they move from the Cascadia Basin into the adjacent subduction zone accretionary prism and experience deformation and consolidation (Westbrook et al., 1994). In this process, pore fluids are expelled and gas, primarily biogenic methane, is transported upward to form hydrates in the upper few hundred meters of the section. An undeformed reference section off Vancouver Island was established

seaward of the prism toe at ODP Site 888. ODP Site 889, where Integrated Ocean Drilling Program (IODP) Expedition 328 operations are planned (Fig. F1A), is located landward of the prism toe where the rate of fluid expulsion, estimated on the basis of rates of thickening and consolidation, reaches a cross-prism maximum. To understand the consolidation, fluid expulsion, and hydrate accumulation and dissociation better, a more complete transect across the prism was drilled during IODP Expedition 311 (Riedel, Collett, Malone, et al., 2006). This work included additional coring, wireline logging, and logging-while-drilling operations in the vicinity of Site 889 at IODP Sites U1327 and U1328 (Fig. F1B). As a result, a total of nine boreholes, along with extensive geophysical site surveys, now provide detailed information about the characteristics of this area and an excellent geophysical, geochemical, and lithologic context for the observatory operations of Expedition 328.

Relevant site characteristics

A simplified schematic cross section in Figure F2 illustrates the way gas hydrates are believed to accumulate in accretionary prisms. Pore fluid expulsion, driven by tectonic thickening and consolidation, is rapid near the prism toe (referred to also as the deformation front) and diminishes landward. Vertical migration of water from the prism delivers small amounts of dissolved methane produced in the sediment by biological CO_2 reduction, to the level of gas hydrate stability (a weak function of pressure and strong function of temperature) where hydrates accumulate primarily in permeable fractures and coarse-grained layers. A discrete boundary between sediments containing free gas and gas hydrate in the sediment pore volume eventually develops. This boundary is seen clearly in seismic sections as a bright reflection (the bottom-simulating reflector, or BSR) at a generally uniform depth below the seafloor (a consequence of its depth being primarily temperature controlled), with a polarity opposite to that from the seafloor (Fig. F3).

The seismic reflection profiles crossing Site 889 also provide a clear image of the local sediment structure, which comprises a gently deformed sequence of slope basin deposits draped over highly deformed accretionary prism sediments. These lithologic units have been characterized in detail by coring and logging at the numerous holes drilled in the immediate vicinity of Site 889 (Fig. F4) (Westbrook et al., 1994; Riedel, Collett, Malone, et al., 2006; Riedel et al., in press). The gas/gas hydrate interface was intersected within the deformed prism unit at a depth of 225 meters below seafloor (mbsf). Hydrates above the interface appear to be virtually absent in fine-grained material; most of the hydrate is concentrated in permeable coarse-grained units and mas-

sive hydrate lenses that mark present or past pathways of focused fluid flow. Minor quantities of free gas are inferred to occur in an interval a few tens of meters below the interface.

Previous attempt to establish a CORK observatory

During Leg 146, two attempts were made to establish Circulation Obviation Retrofit Kit (CORK) hydrologic observatories, one at Site 889 and the other in a similar setting at ODP Site 892 off central Oregon (Westbrook et al., 1994; Davis et al., 1995). These were equipped with sensors to monitor temperatures at multiple formation levels and pressure at the level of perforations in a liner extending below casing. The installation at Hole 892B was successful and operational for roughly 2 y before the instrumentation was removed to facilitate fluid sampling. Owing to unstable formation conditions and deteriorating weather, the installation in Hole 889C did not succeed. Instability of the formation caused sediment to be squeezed into the casing through the perforations, the open end of the liner, and/or the annulus between the liner and the casing (Fig. F5). This prevented the thermistor cable from reaching its intended depth, which in turn precluded a pressure-tight seal of the pressure logging system at the top of the hole. The total hole depth was 385 mbsf; the bottom of the liner was at 323 mbsf; after two aborted attempts to deploy the thermistor cable, a sinker-bar run indicated fill had reached 253 mbsf; the failed third attempt with a cable shortened to 240 m suggested that sediment had intruded the casing up to this depth. The CORK was never refurbished.

Observatory objectives and design

Motivation

As a result of this failure, the objectives of the CORK monitoring planned for Leg 146, namely to document the average pressure state of the prism created by tectonic strain and gravitational loading, the pressure gradient driving fluid expulsion and gas migration, and the thermal profile as a constraint on the vertical velocity of interstitial fluid flow, have never been met; hence, they continue to provide motivation for an observatory installation at Site 889. In addition, many advances have been made with monitoring experiments in other settings since the time of Leg 146 nearly 18 y ago, and these provide new elements of motivation. From a scientific perspective, long-term monitoring experiments at a number of sites in tectonically active settings (Juan

de Fuca Ridge axis and flank, Mariana forearc prism, Costa Rica forearc prism, and Nankai accretionary prism) have revealed that formation pressure variations provide a quantitative proxy for volumetric strain. Transient events related to coseismic, postseismic, and aseismic deformation have been seen at all of these locations, and the observations are leading to a new understanding about the episodic nature of deformation, seismic energy efficiency, and regional interseismic strain accumulation. An example from the Nankai Trough (Fig. F6) shows the pressure response to coseismic, postseismic, and secular interseismic strain. With the relatively high frequency recording and precise timing possible with a NEPTUNE cable connection and the high resolution provided by current sensor technology, it is also possible to observe formation strain associated with seismic ground motion. This has been documented in numerous instances (Fig. F7).

We anticipate that signals similar to these examples will be present at Cascadia. An illustration of the likelihood of their presence is provided by the combination of Figures F8, F9, F10, and F11. Figure F8 shows Site 889 to be surrounded by high seismic activity. To the northwest of the site, strike-slip events are concentrated along the Nootka fault, the strike-slip boundary between the Juan de Fuca and Explorer oceanic plates. Along the continental margin, intraplate events occur in the overriding continental crust and in the oceanic crust of the subducting Juan de Fuca and Explorer plates (Fig. F8A). Further landward, seismic tremor occurs episodically along and above the top of the subducting plate, downdip of the thrust seismogenic zone (Fig. F8B). No events have yet been identified on the currently "locked" part of the subduction thrust interface, although in other subduction zone settings (Nankai and Costa Rica), slow slip crossing the "locked zone" has been documented (Davis and Villinger, 2006; Heesemann and Davis, submitted). Figure F9 demonstrates the utility of using pressure as a proxy for strain by way of the reaction at a CORKed site on the nearby Juan de Fuca Ridge flank to two seismogenic strain events 100 to 150 km away. The recurrence statistics of intraplate and Nootka fault earthquakes within 150 km of Hole 889C (Fig. F10) and the regular occurrence of slip events downdip of the locked portion of the subduction thrust (Fig. F11) show that strain-related signals and instances of formation pressure response to seismic ground motion should be plentiful in a relatively short period of time.

Beyond these scientific considerations, a number of technical factors fortify the justification for a geophysical observatory at this site. The high reliability of CORK instrumentation has been demonstrated through successful long-term operations at many sites. Instruments deployed during ODP Leg 196 (Nankai Trough) have been operat-

ing for >7 y, and those deployed during ODP Legs 168 and 169 have been in operation for >13 y. Improvements in power consumption, memory capacity, and resolution now permit detection of much subtler signals than were previously possible. And in this instance, connection to the NEPTUNE observatory cable infrastructure will open up great opportunities. Much higher sampling frequency will be achieved, allowing observations to reach into the seismic frequency band (Fig. F7) and to be placed in context of colocated seismic and hydrologic records that are being collected with a broadband seismometer and a variety of seafloor vent monitoring instruments roughly 3.5 km from the Site 889 Advanced CORK (ACORK) borehole observatory.

Observatory configuration

Most CORK installations to date have been configured to meet a broad suite of requirements, including passive geophysical monitoring, active hydrologic testing, and formation-fluid chemical and microbiological sampling (see reviews by Kastner et al., 2006; Becker and Davis, 2005; Fisher et al., 2005). Unfortunately, large perturbations can occur when fluids are allowed to be produced from the formation, particularly when monitoring screens are situated in low-permeability material. Direct effects arise from any pressure drop associated with production, and indirect effects arise from thermal perturbations caused by flow (see discussion in Davis and Becker, 2007). The latter can be caused by the anomalous buoyancy of the water in the umbilical screens that connect to the seafloor sensors and from transient thermal expansion of the fluid in the umbilical and screens that is confined by the low-permeability material surrounding the screens. To avoid these problems, this observatory will be devoted to passive geophysical monitoring exclusively; fluid sampling and active experiments, specifically those proposed in Proposal 553-Full2 (www.iodp.org/597/), will be carried out at a later date in separate holes. It is our hope that justification for paired monitoring and sampling holes will be provided by the early results of this expedition's passive monitoring effort; we anticipate that the Expedition 328 efforts will be neither redundant nor conflicting but fully complementary with those of a more extensive future program.

The primary components of the ACORK system to be deployed are shown in Fig. F12. Four screens will be centered at depths of 155, 205, 245, and 295 mbsf; two are above and two are below the gas/gas hydrate boundary at 225 mbsf, and all are within the accretionary prism lithologic unit (Fig. F4). Screens will be virtually identical to those used for Leg 196, with 7.6 m long sections of filter screens built on standard 11.24 m long 10¾ inch diameter solid casing joints. Carbolite (aluminum oxide ceramic)

"sand" is packed in the ~2 cm annulus between the casing and a screen formed of wire wrapped around and welded to radial webs.

Formation pressure signals are transmitted to seafloor sensors via ¼ inch outer diameter 0.035 inch wall 316 stainless steel umbilical tubing. Packers between screens will not be used at Site 889; based on results from the ACORK at ODP Site 808 and previous experience at Site 889, we are confident that hole collapse will provide a good seal between the ACORK casing and the formation.

Pressure monitoring instruments will be installed in the wellhead frame on the ship and deployed with the ACORK casing string. Underwater-mateable hydraulic connectors will allow the instrument package to be removed and replaced in the event that repairs or service are ever required. Gas will be purged from the umbilical tubing through lockable check valves at the highest point of the wellhead plumbing. Three-way valves will connect the umbilical lines to the instrumentation: in the "formation" position, these will connect the formation to the sensors; in the "hydrostatic" position, the formation lines will be closed and the sensors will be connected to the local ocean. The logging instrumentation will include individual sensors (Paroscientific 8B 4000-2 quartz transducers) to monitor pressures at the seafloor and at each of the formation screens. Frequency output from these will be digitized with high-resolution (~10 ppb full scale = 0.4 Pa) low-power "Precision Period Counter" cards (Bennest Enterprises, Ltd.), and stored in MT-01 flash memory (Minerva Technologies, Ltd.). The records shown in Figure F7 were recorded by an identical unit. Bottom water temperature will be determined from a temperature-sensitive frequency channel of the Paroscientific sensors and with a highly stable platinum thermometer. Battery capacity will be sufficient to power the system for roughly 10 y at a sampling period of 10 s. An onboard voltage detection circuit will switch the system into a high-rate (1 Hz) sampling mode and idle the batteries when external power from a NEPTUNE connection is made (anticipated within the first year of operation).

At the top of the ACORK wellhead structure will be a ~30 inch diameter reentry cone, needed for installation of the bridge plug in the 10¾ inch casing. This will later facilitate submersible-controlled wireline installation of deep instrument packages, including a thermistor cable, tilt sensors, and a seismometer for low-frequency seismology.

Screen spacing

The rationale for the ACORK screen configuration deserves some discussion. At the simplest level, multiple monitoring points will allow determinations of the average vertical pressure gradient generated by prism thickening and driving vertical fluid flow and the contrast in gradient between the section above and below the level of gas hydrate stability associated with a contrast in permeability if one exists. The combination of the 7.6 m length of the screens and their ~50 m separation should make such gradient determinations relatively insensitive to localized heterogeneities associated with fractures, turbidite layering, and lenses of massive hydrate accumulation.

Data from below and above the gas/gas hydrate boundary will also constrain the contrast in mechanical properties of gas and gas hydrate–bearing sediments and provide independent information about the effective permeabilities of the sections above and below the boundary. The way this can be done is summarized in Figure F13, which begins with a schematic illustration of how variable loading either at the seafloor (e.g., tides and ocean waves) or within the formation (tectonic strain and seismic waves) is transmitted to formation pore water and how local contrasts in loading response causes transient pressure gradients to be established (Fig. F13A). The instantaneous (elastic) response to seafloor loading = γ (referred to as the loading efficiency) (Fig. F13B) depends on porosity, Poisson's ratio, the compressibility of the solid grain constituents, the compressibility of the sediment or rock framework, and the compressibility of the interstitial fluid or fluid + gas mixture. With the first three of these being well known, absolute values and contrasts in observed loading efficiency can be used to constrain the effects of gas on the elastic properties of the fluid (and hence gas content) and the effect of hydrates on the elastic properties of the matrix (and hence average hydrate content).

In simple cases where a sharp mechanical properties contrast is present (e.g., at the seafloor or at the gas/gas hydrate boundary), a transient pressure gradient will be established and interstitial water will flow (Fig. F13A). A damped diffusional wave will propagate away from the boundary, adding a component to the signal (Fig. F13B) that decays with distance (Fig. F13C). At large distances, the response is purely elastic (γ) and constrains such things as the matrix compressibility, the gas content (Fig. F13D), and the coefficient that defines how tectonic deformation loads the interstitial water (Fig. F13E). At intermediate distances, the characteristic diffusion scale length, l, (Fig. F13C) depends on the hydraulic diffusivity of the formation, η, and the period of the loading signal, P, as $l = (\pi \eta P)^{1/2}$. The broad bandwidth of ocean wave and tidal load-

ing, for which periods range from seconds to weeks, combined with the distribution of the screens around the gas/gas hydrate boundary, should allow much to be learned about the formation elastic and hydrologic properties.

Schedule for Expedition 328

Expedition 328 is based on Integrated Ocean Drilling Program drilling proposal number 734-APL (available at **iodp.tamu.edu/scienceops/expeditions/cascadia.html**). Following ranking by the IODP Scientific Advisory Structure, the expedition was scheduled for the research vessel *JOIDES Resolution*, operating under contract with the U.S. Implementing Organization. At the time of publication of this *Scientific Prospectus*, the expedition is scheduled to start in Victoria, Canada, on 4 September 2010 and to end in Victoria, Canada, on 18 September 2010. A total of 6 days is scheduled for activities on site, with 0.6 day transits from and to Victoria (for the current detailed schedule, see **iodp.tamu.edu/scienceops/**). Further details about the facilities aboard the *JOIDES Resolution* and at the USIO can be found at **www.iodp-usio.org/.**

Operations plan

Up to five pipe trips will be required to complete the following steps of the ACORK installation:

1. A jet-in test to determine the depth to set load-bearing conductor casing (tentative),
2. Conductor casing and reentry-cone installation,
3. Drilling to a total depth of 315 mbsf,
4. Installation of the ACORK casing string with operational wellhead pressure monitoring instrumentation,
5. Installation of a bridge plug, and
6. Deployment of a remotely operated vehicle (ROV)/submersible landing platform.

Details of the operations plan and a breakdown of time estimates are provided in Table **T1.**

Based on previous drilling experience at this location, it is anticipated that four joints of 16 inch conductor casing will be required. The 10¾ inch ACORK casing and its

screens will be deployed in the open hole below this with the help of an underreamer, which will have been used during the previous expedition. The ACORK casing will hang in the 16 inch conductor casing from a landing flange at the base of the reentry cone. To maximize the hydraulic resistance between the uppermost screen and the seafloor, a swellable packer will be employed at the top of the ACORK casing string to seal the anulus between the 10¾ inch and 16 inch casings. The bottom-hole seal for the 10¾ inch ACORK casing has not yet been selected. Two possibilities are a mechanical-set bridge plug (rotationally or hydraulically activated) and a swellable packer (positively latched to withstand formation overpressure). Use of cement is also being considered to augment this critical seal.

Risks and contingencies strategy

We hope that previous drilling experience at this site will allow risks to be anticipated and planned for. Difficulties arising from hole instability are considered unlikely, but if encountered they can be overcome with aggressive use of the underreamer. Difficulties were encountered with reaching target depths with ACORK installations in ODP Holes 808I and 1173B, but they appear to have been due in large part to failure of the undereamer bit used. Similar problems for Expedition 328 are not anticipated; a more robust bit will be used, and the casing completion depth is much less (300 mbsf at Site 889 versus 750 and 930 mbsf at Sites 808 and 1173, respectively). Integrity of the internal seal in the 10¾ inch casing is crucial for the success of the pressure monitoring experiment, and placement of the seal at the bottom of the casing string is of utmost importance for later experiments that require instruments to be installed deep inside the sealed casing. Correct choice of the hardware to achieve a tight seal at depth is critical.

References

Becker, K., and Davis, E.E., 2005. A review of CORK designs and operations during the Ocean Drilling Program. *In* Fisher, A.T., Urabe, T., Klaus, A., and the Expedition 301 Scientists, *Proc. IODP,* 301: College Station, TX (Integrated Ocean Drilling Program Management International, Inc.). **doi:10.2204/iodp.proc.301.104.2005**

Davis, E., and Becker, K., 2007. On the fidelity of "CORK" borehole hydrologic observatory pressure records. *Sci. Drill.,* 5:54–59. **doi:10.2204/iodp.sd.5.09.2007**

Davis, E.E., Becker, K., Wang, K., and Carson, B., 1995. Long-term observations of pressure and temperature in Hole 892B, Cascadia accretionary prism. *In* Carson, B., Westbrook, G.K., Musgrave, R.J., and Suess, E. (Eds.), *Proc. ODP, Sci. Results,* 146 (Pt. 1): College Station, TX (Ocean Drilling Program), 299–311. **doi:10.2973/odp.proc.sr.146-1.219.1995**

Davis, E., Becker, K., Wang, K., and Kinoshita, M., 2009. Co-seismic and post-seismic pore-fluid pressure changes in the Philippine Sea plate and Nankai decollement in response to a seismogenic strain event off Kii Peninsula, Japan. *Earth, Planets Space,* 61:649–657.

Davis, E.E., and Villinger, H.W., 2006. Transient formation fluid pressures and temperatures in the Costa Rica forearc prism and subducting oceanic basement: CORK monitoring at ODP Sites 1253 and 1255. *Earth Planet. Sci. Lett.,* 245(1–2):232–244. **doi:10.1016/j.epsl.2006.02.042**

Davis, E.E., Wang, K., Becker, K., and Thomson, R.E., 2000. Formation-scale hydraulic and mechanical properties of oceanic crust inferred from pore pressure response to periodic seafloor loading. *J. Geophys. Res.,* 105(B6):13423–13436. **doi:10.1029/2000JB900084**

Davis, E.E., Wang, W., Thomson, R.E., Becker, K., and Cassidy, J.F., 2001. An episode of seafloor spreading and associated plate deformation inferred from crustal fluid pressure transients. *J. Geophys. Res.,* 106(B10):21953–21964. **doi:10.1029/2000JB000040**

Fisher, A.T., Wheat, C.G., Becker, K., Davis, E.E., Jannasch, H., Schroeder, D., Dixon, R., Pettigrew, T.L., Meldrum, R., McDonald, R., Nielsen, M., Fisk, M., Cowen, J., Bach, W., and Edwards, K., 2005. Scientific and technical design and deployment of long-term, subseafloor observatories for hydrogeologic and related experiments, IODP Expedition 301, eastern flank of Juan de Fuca Ridge. *In* Fisher, A.T., Urabe, T., Klaus, A., and the Expedition 301 Scientists, *Proc. IODP,* 301: College Station, TX (Integrated Ocean Drilling Program Management International, Inc.). **doi:10.2204/iodp.proc.301.103.2005**

Heesemann, M., and Davis, E.E., submitted. New evidence for episodic aseismic slip across the seismogenic zone off Costa Rica: CORK formation pressure transients at ODP Sites 1253 and 1255. *Nature (London, U. K.).*

Hyndman, R.D., and Davis, E.E., 1992. A mechanism for the formation of methane hydrate and seafloor bottom-simulating reflectors by vertical fluid expulsion. *J. Geophys. Res.,* 97:7025–7041.

Kao, H., Shan, S.-J., Dragert, H., Rogers, G., Cassidy, J.F., Wang, K., James, T.S., and Ramachandran, K., 2006. Spatial-temporal patterns of seismic tremors in northern Cascadia. *J. Geophys. Res., [Solid Earth],* 111(B3):B03309. **doi:10.1029/2005JB003727**

Kastner, M., Becker, K., Davis, E.E., Fisher, A.T., Jannasch, H.W., Solomon, E.A., and Wheat, G., 2006. New insights into the hydrogeology of the oceanic crust through long-term monitoring. *Oceanography,* 19(4):46–57.

Riedel, M., Collett, T.S., Malone, M.J., and the Expedition 311 Scientists, 2006. *Proc. IODP,* 311: Washington, DC (Integrated Ocean Drilling Program Management International, Inc.). **doi:10.2204/iodp.proc.311.2006**

Riedel, M., Collett, T.S., and Malone, M., in press. IODP Expedition 311—scientific findings. *In* Riedel, M., Collett, T.S., Malone, M.J., and the Expedition 311 Scientists, *Proc. IODP,* 311: Washington, DC (Integrated Ocean Drilling Program Management International, Inc.).

Rogers, G., and Dragert, H., 2003. Episodic tremor and slip on the Cascadia subduction zone: the chatter of silent slip. *Science,* 300(5627):1942–1943. **doi:10.1126/science.1084783**

Wang, K., and Davis, E.E., 1996. Theory for the propagation of tidally induced pore pressure variations in layered subseafloor formations. *J. Geophys. Res.,* 101(B5):11483-11496. **doi:10.1029/96JB00641**

Wang, K., Davis, E.E., and van der Kamp, G., 1998. Theory for the effects of free gas in subsea formations on tidal pore pressure variations and seafloor displacements. *J. Geophys. Res.,* 103(B6):12339–12354. **doi:10.1029/98JB00952**

Westbrook, G.K., Carson, B., and Shipboard Scientific Party, 1994. Summary of Cascadia drilling results. *In* Westbrook, G.K., Carson, B., Musgrave, R.J., et al., *Proc. ODP, Init. Repts.,* 146 (Pt. 1): College Station, TX (Ocean Drilling Program), 389–396. **doi:10.2973/odp.proc.ir.146-1.012.1994**

Table T1. Expedition 328 operations plan. (**See table notes.**)

Site No.	Location (Latitude Longitude)	Sea Floor Depth (mbrf)	Operations Description	Transit (days)	Ops (days)	Log (days)
			Start Expedition in Victoria, B.C., Canada　　4-Sep-10	In Port	(5 Days)	
			Transit ~141 nmi to Site TBD (close to Site 889) @ 10.5 kt	0.6		
CAS-01CORK	48° 41.9964' N	1326	RIH & jet-in new reentry cone with 4 jts of 16" casing (~56m)		6.0	0.0
	126° 52.3302' W		RT pipe, reenter, drill 14-3/4" hole to 315 mbsf,			
			Displace hole w/heavy mud & POOH,			
			Make-up ACORK, RIH w A-CORK, bit, & UR asbly, reenter & land ACORK,			
			(ACORK consists of 4ea screened joints w/10-3/4" csg)			
			Displace hole with heavy mud & set cement plug at base of 10-3/4" ACORK			
			POOH, deploy CORK platform, POOH			
			Sub-Total Days On-Site:　　6.0			
			Transit ~148 nmi to Victoria, B.C. @ 10.5 kt	0.6		
			End Expedition in Victoria, B.C., Canada　　18-Sep-10	1.2	6.0	0.0

Subtotal On-Site Time:	6.0
Total Operating Days:	7.2
Total Expedition Including (5.0 day) Port Call:	12.2

Notes: Seafloor depth is prospectus water depth plus 11.0 m adjustment from water line to rig floor (i.e. drillers depth). RIH = run in hole, RT = running tool, POOH = pull out of hole, UR = underreamer.

Figure F1. Maps showing (**A**) regional and (**B**) local context of ODP Site 889 and IODP Expedition 328 operations. The ACORK observatory will be located 200 m northwest of Hole 889C along Inline 35. (**Continued on next page.**)

A
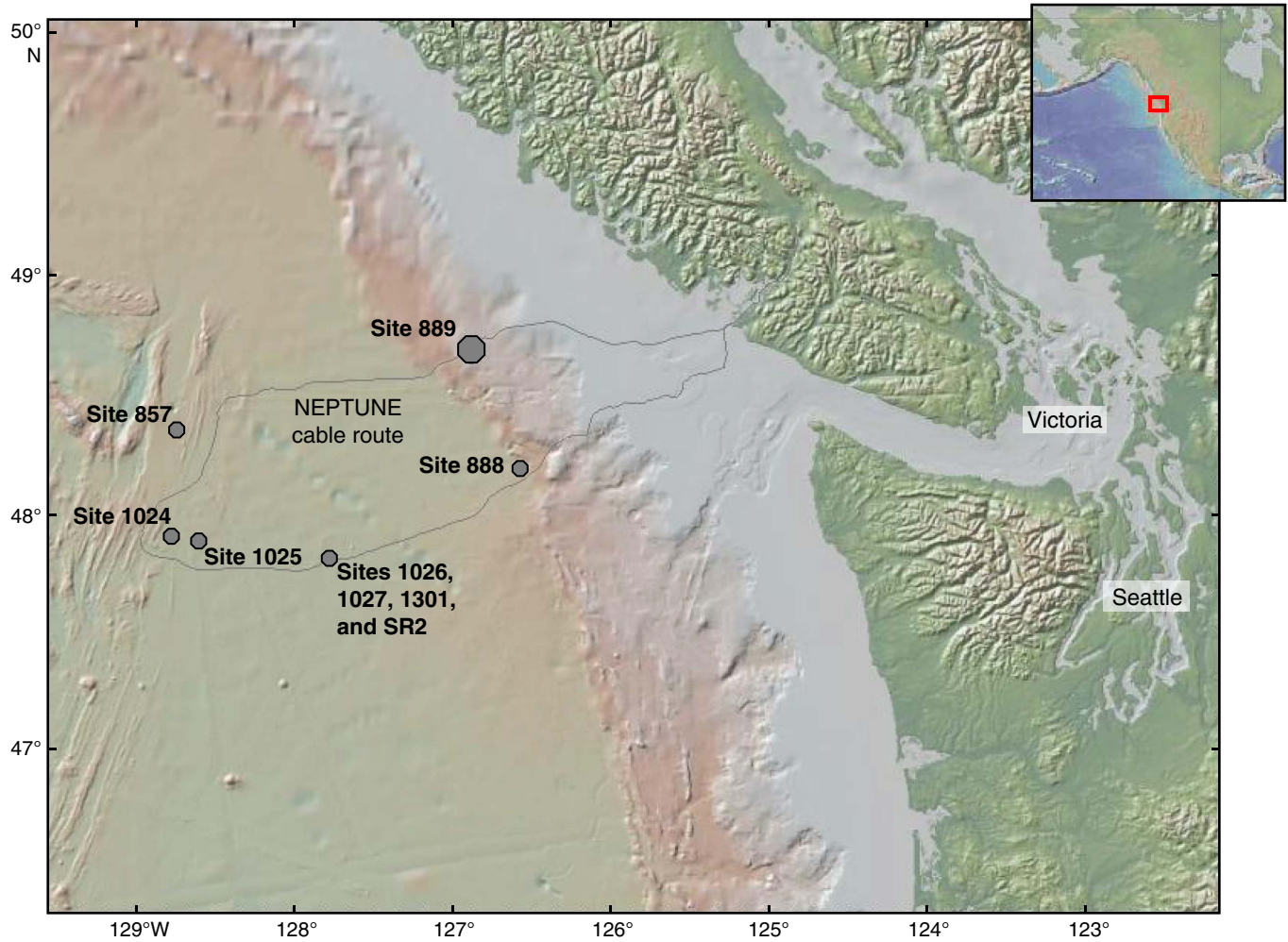
Figure F1 (continued).

B
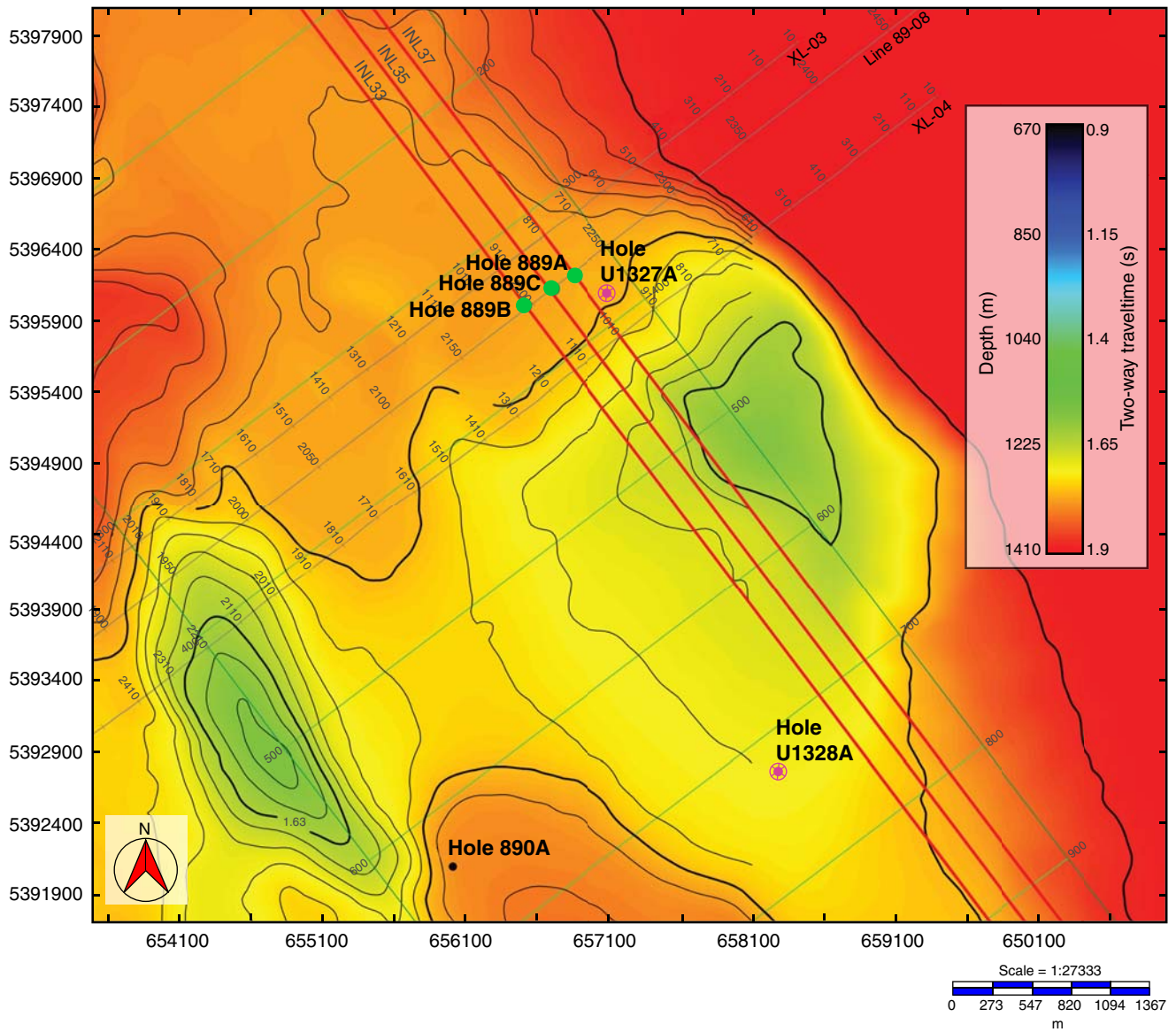
Figure F2. Schematic showing basic processes thought to be important in the formation of gas hydrates in accretionary prism sediments above the predominantly temperature-sensitive limit of hydrate stability (from Hyndman and Davis, 1992). BSR = bottom-simulating reflector.
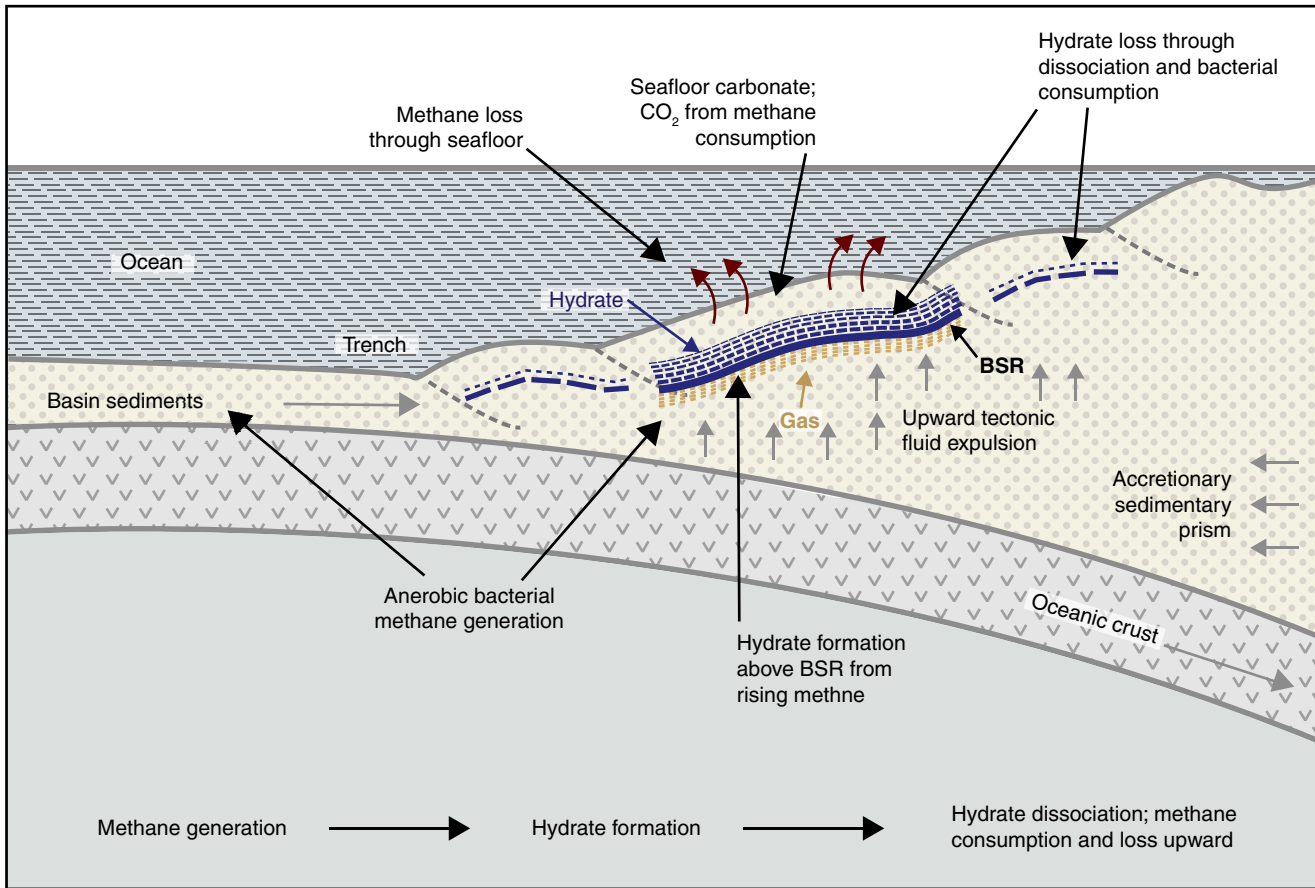
Figure F3. (A) Multichannel and single-channel seismic lines (B) along and (C) across the accretionary prism in the vicinity of ODP Site 889, showing gently deformed slope-basin deposits overlying highly deformed accretionary prism sediments and the bottom-simulating reflector (BSR) that marks the limit of gas hydrate stability (from Riedel, Collett, Malone, et al., 2006). SP = shotpoint. (**Continued on next two pages.**)

A

Expedition 328 Scientific Prospectus

B

Dip Line XL-03
SW → NE

Expedition 328 Scientific Prospectus
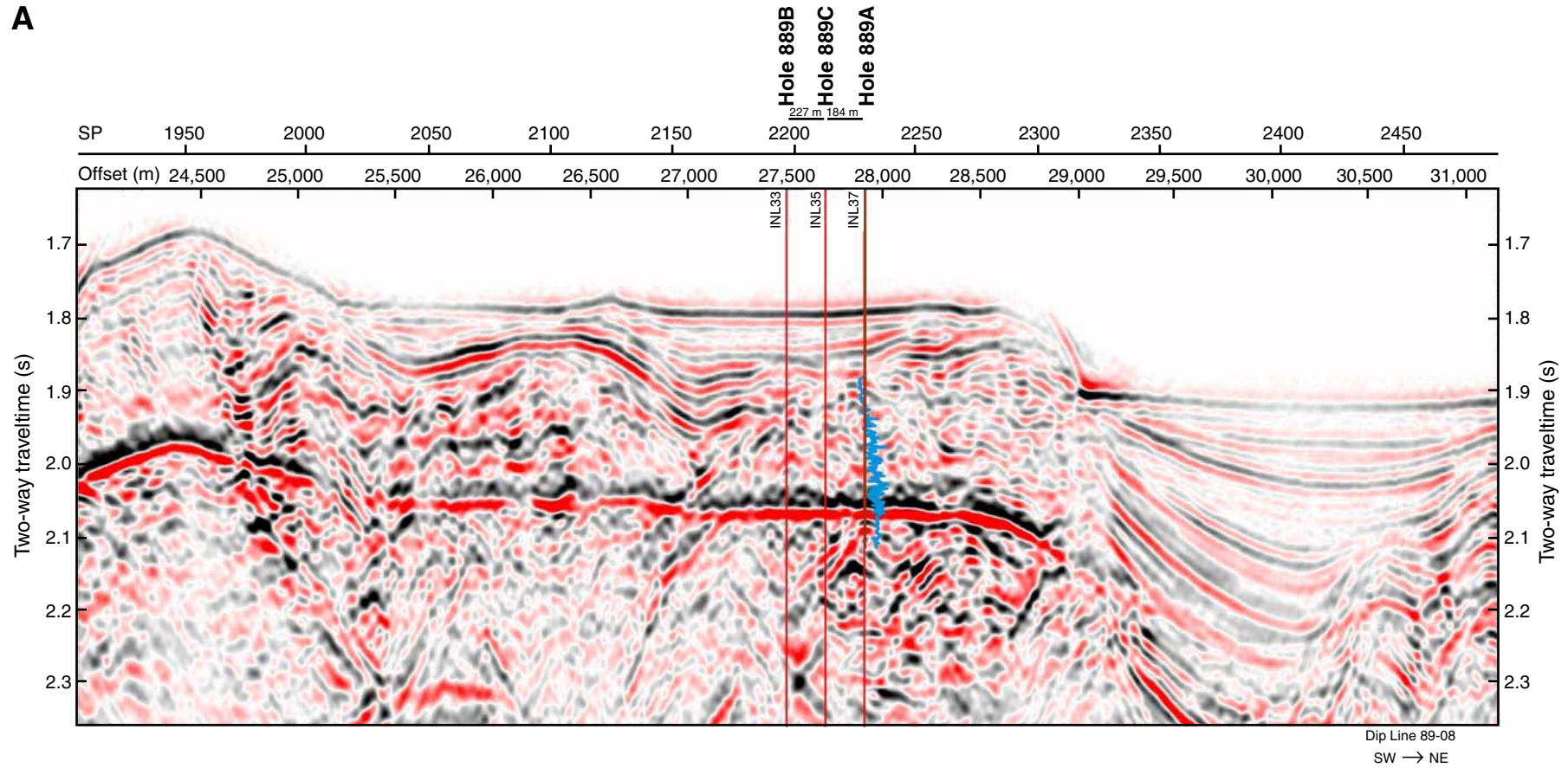
Figure F3 (continued).

Expedition 328 Scientific Prospectus
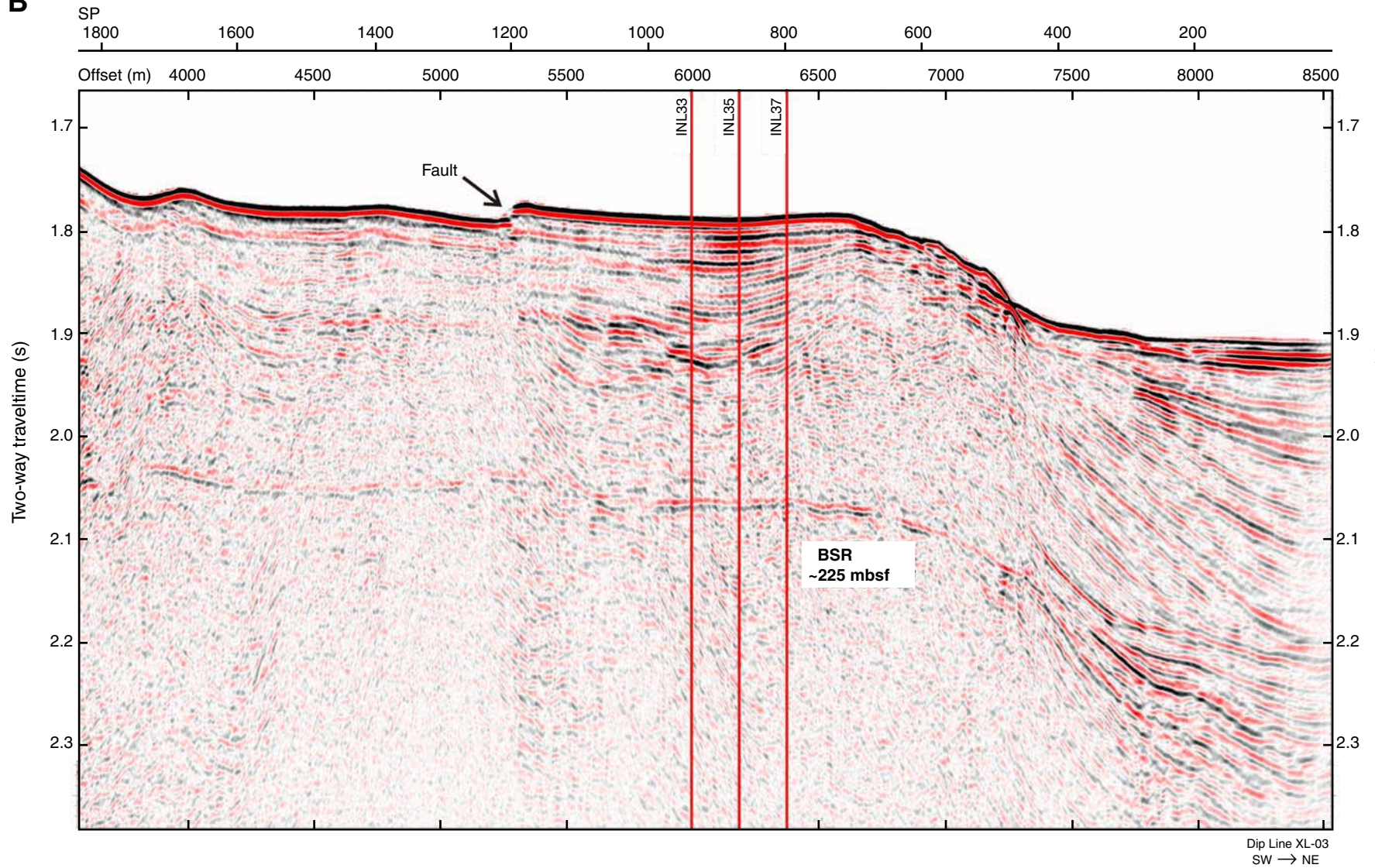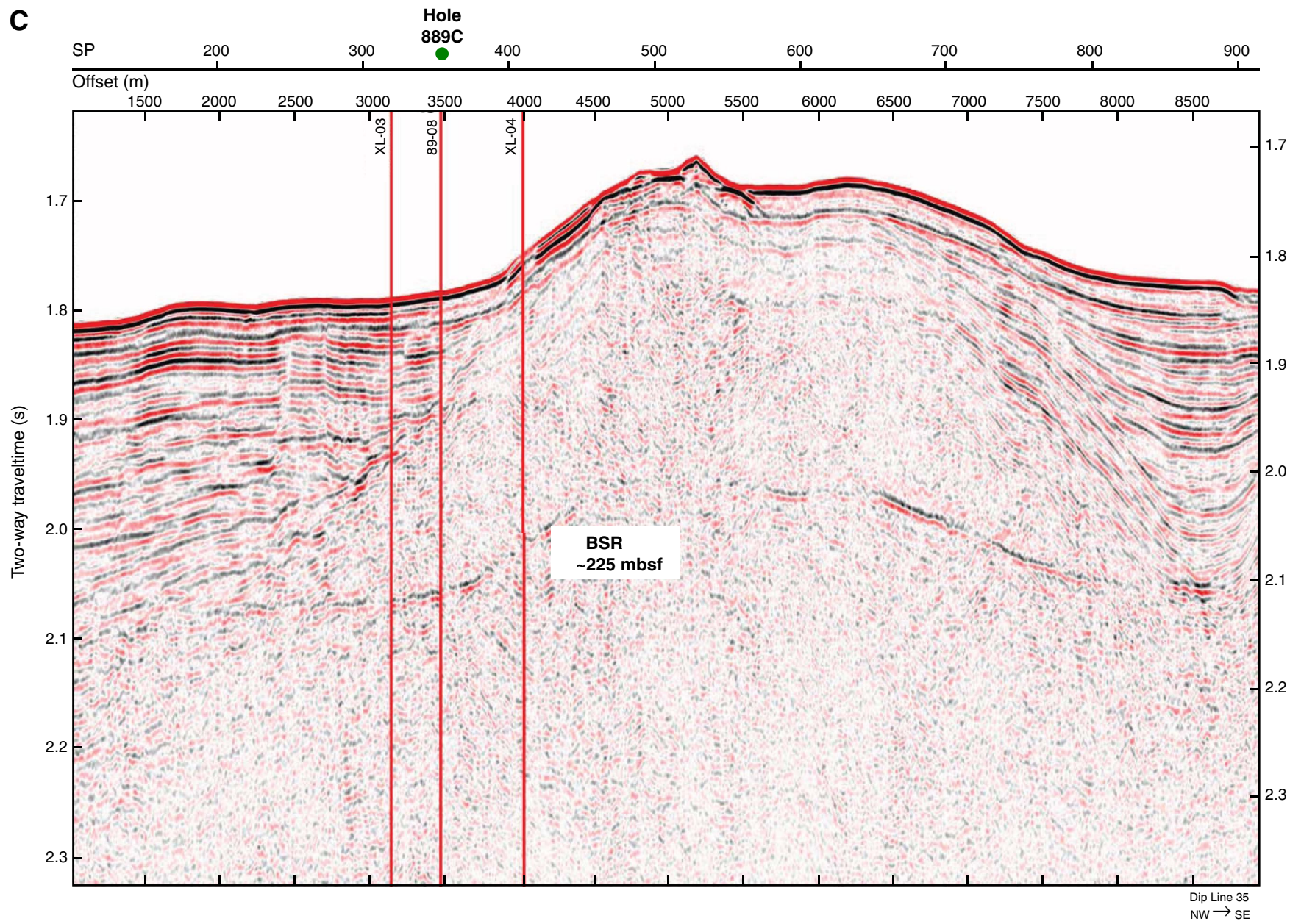
Figure F4. Summary of Site 889 lithology (after Riedel, Collett, Malone, et al., 2006), with screen positions shown as green symbols on the seismic section. BSR = bottom-simulating reflector.
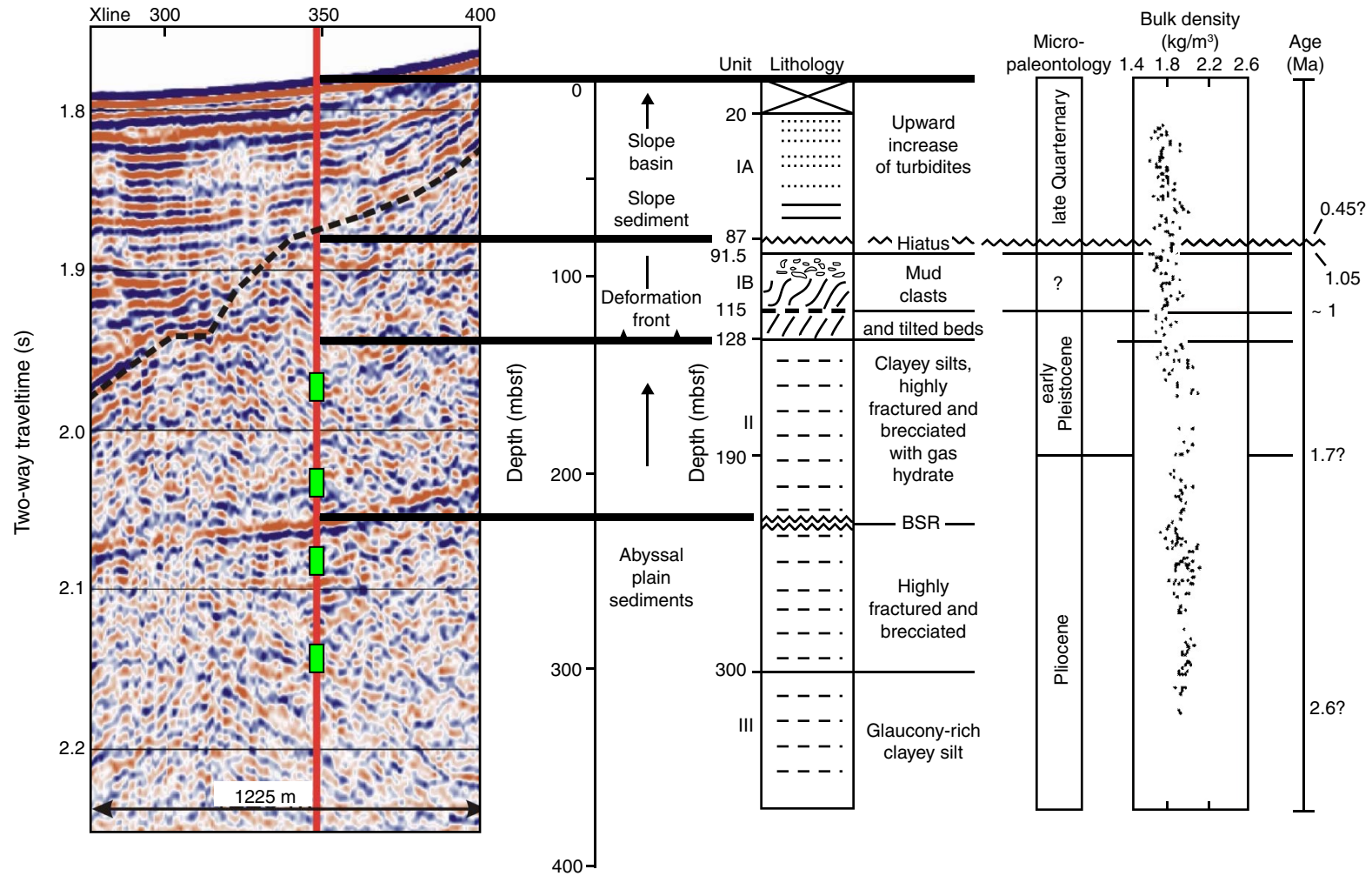
Figure F5. Schematic diagram of CORK installed in Hole 889C during ODP Leg 146. Even after shortening the cable by folding, rapidly accumulating fill in the lower part of the hole prevented the cable from being pulled in completely by its sinker bar, which in turn prevented the data logger from fully seating and sealing in the CORK body.
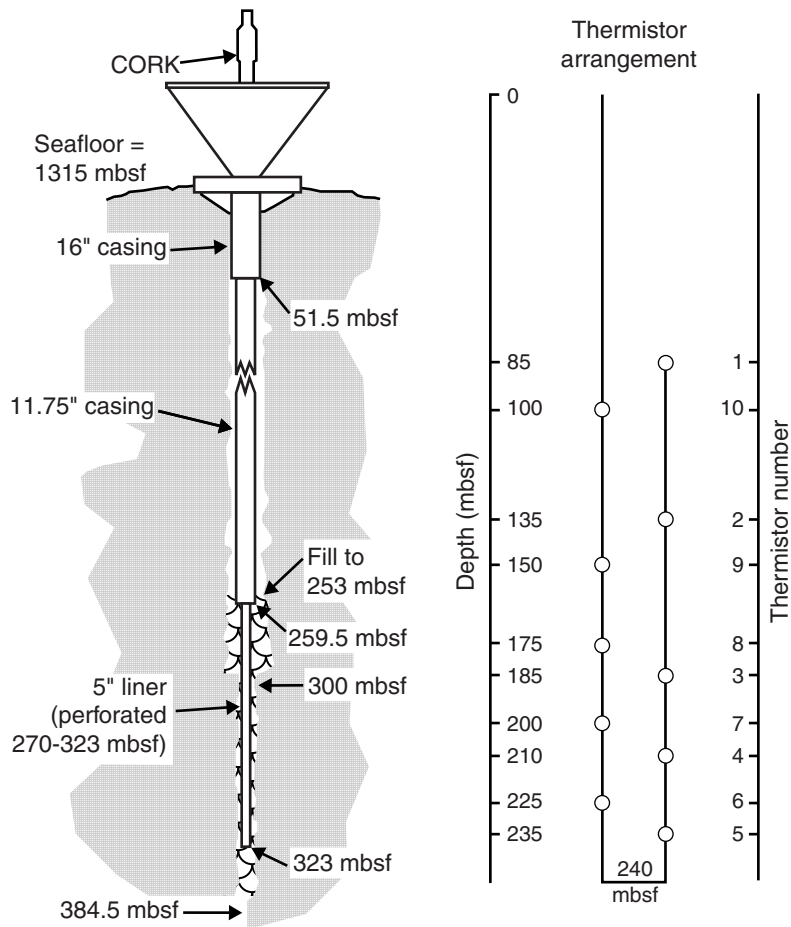
Figure F6. Strain at the time of and following magnitude 7.2 and 7.5 earthquakes beneath the Nankai Trough off Kii Peninsula, Japan (star), reflected in aftershocks in the near vicinity of the earthquake (filled circles in A and B) and in a rise in formation-fluid pressure observed at an ACORK located 220 km from the epicentral area (red line in B). Far-field strain estimated from the seismic moment (volumetric strain shown as contours in A) is far less than inferred from either the coseismic or postseismic pressure increase (secondary axis in B). A smaller but similar signal was observed at the time of a very low frequency earthquake cluster off Cape Muroto (open circles in A) (from Davis et al., 2009). A secular trend of roughly 1.7 kPa/y (0.3 μstrain/y) is also present but has been removed in this plot.
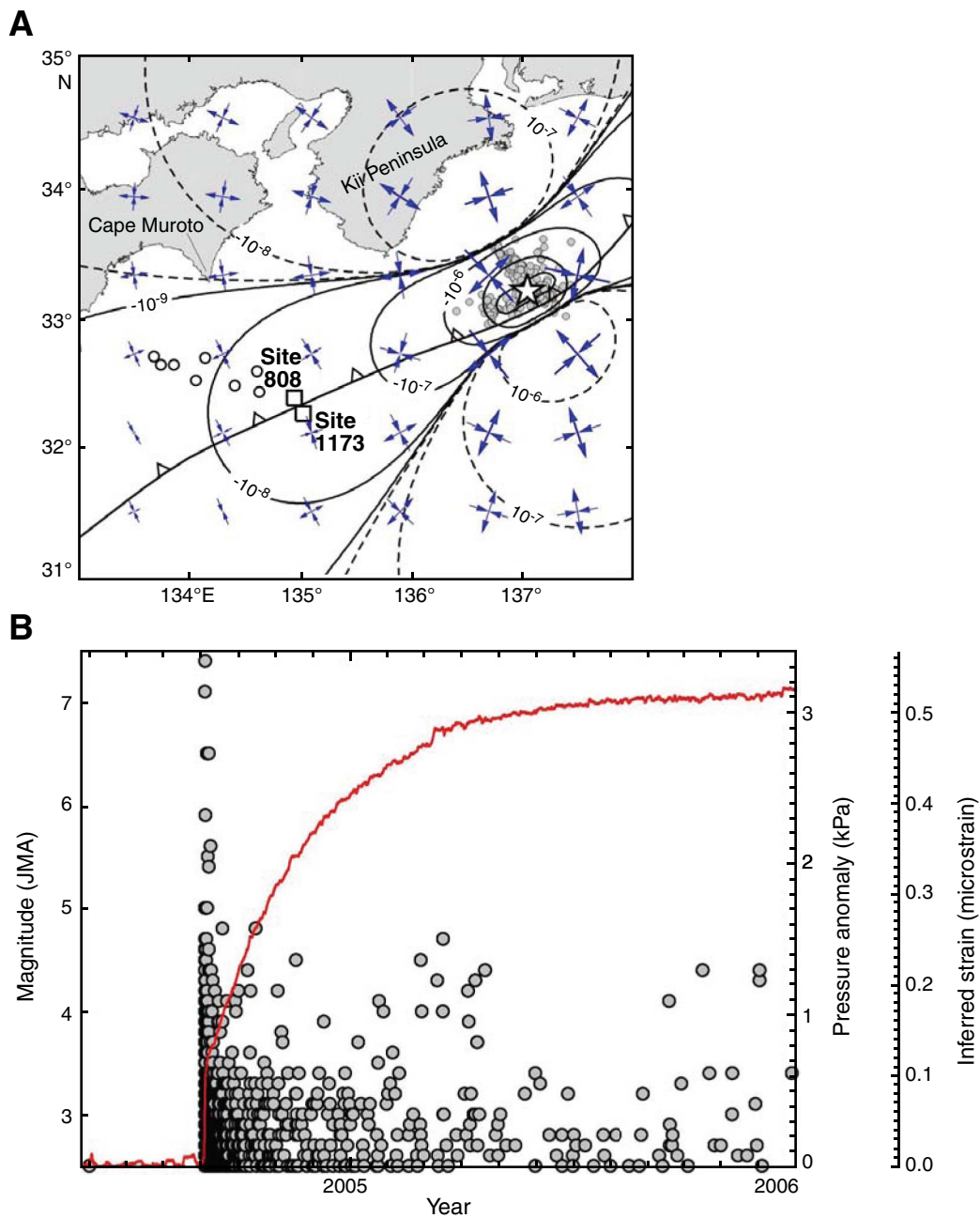
Figure F7. Hydroseismograms for (**A, B**) distant (10 s sampling) and (**C**) local earthquakes (1 Hz sampling using the NEPTUNE cable connection). Comparison of borehole and seafloor signals in A and B shows *P*-waves to be attenuated in the formation relative to the seafloor by the same amount as the tidal loading signal, whereas the seismic Rayleigh waves produce large pressure signals in the formation. The remarkable match of the seafloor pressure record in C with that of a nearby broad-band seismometer (blue and red traces, respectively) demonstrates the high fidelity of recording afforded with the NEPTUNE connection, allowing both high-frequency oceanographic (e.g., before the earthquake) and low-frequency seismic loading to be studied.
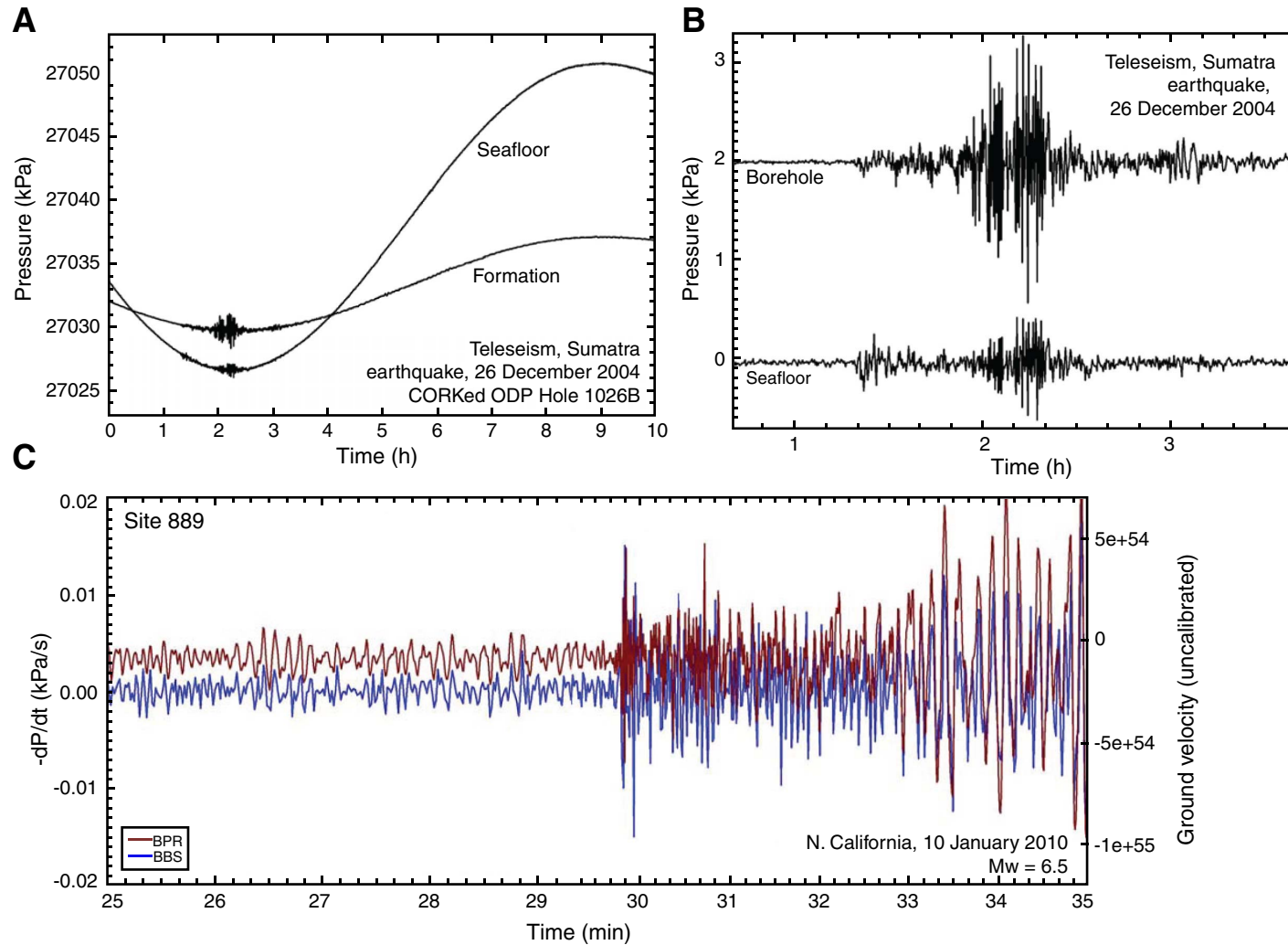
Figure F8. Seismicity along the northern Cascadia region in the vicinity of Site 889 (red circle). Earthquakes in oceanic and continental crust are shown as black and blue symbols in **A,** and tremor events at and above the subduction thrust boundary are shown as red symbols in **B.** Stars = large continental crustal events. No events have been detected with the land-based seismic network on the subduction thrust seaward of the band of tremor events (i.e., where the thrust is believed to be locked during the current phase of a several-hundred-year-long interseismic interval) (from Kao et al., 2006). ETS = episodic tremor and slip.
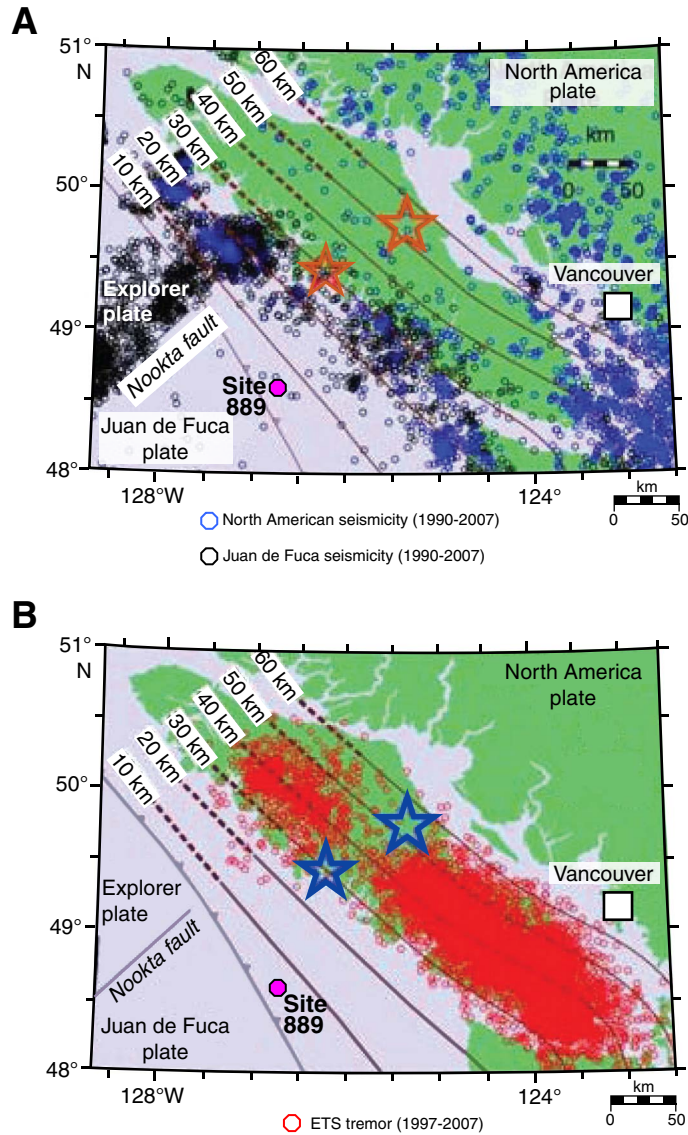
Figure F9. Strain, reflected in formation pressure changes in Hole 1027C on the flank of the Juan de Fuca Ridge, following two seismogenic slip events (red stars) near the ridge axis. The sense of strain (expansive in **A**, contractional in **B**) is in each case consistent with that predicted on the basis of the earthquake moment tensors. The CORK observatory in this hole is completed in highly permeable oceanic crust; lateral drainage from beneath the low-permeability sediment cover causes eventual drainage of the anomalous pressure. (After Davis et al., 2001.)
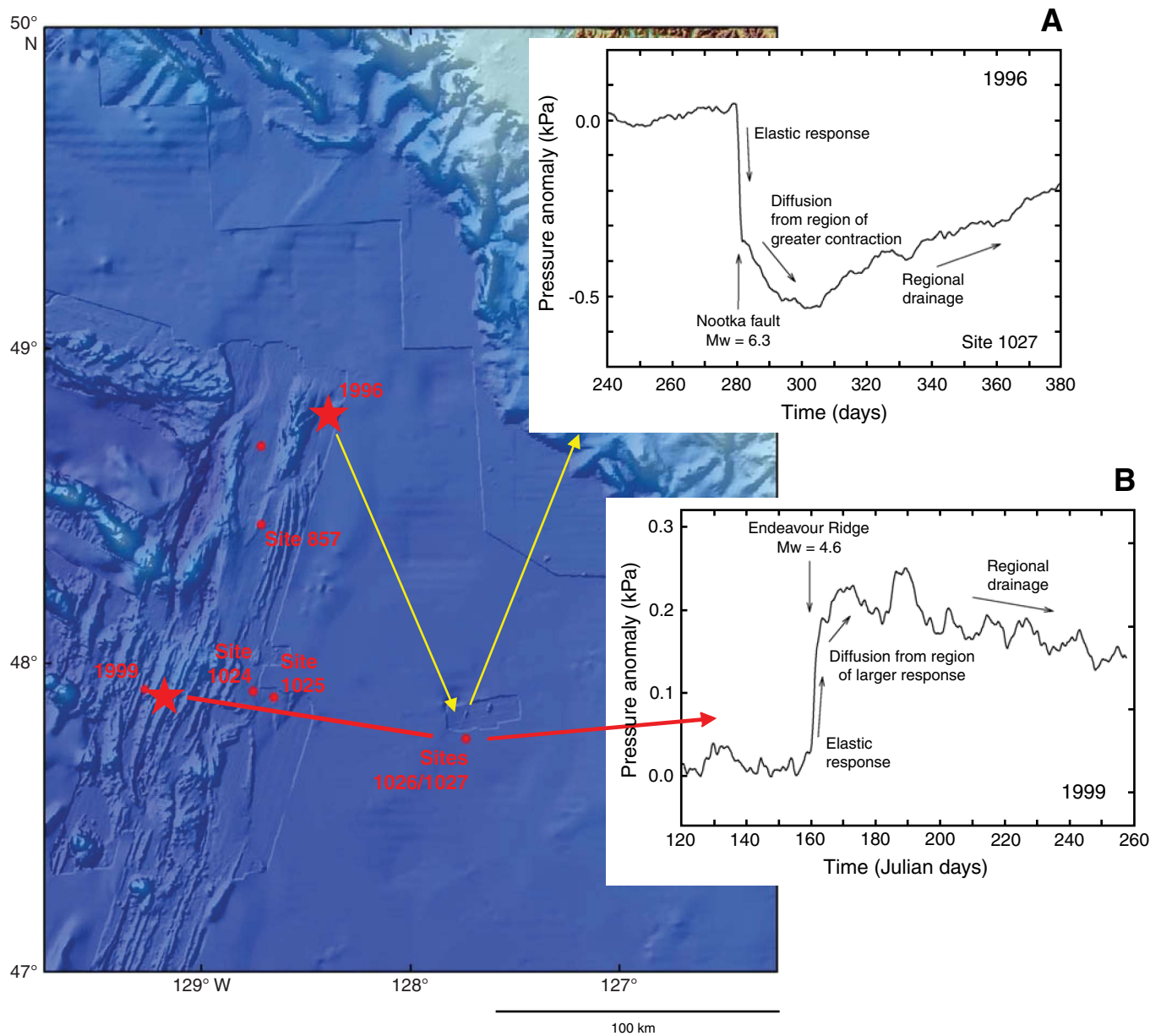
Figure F10. Recurrence statistics for earthquakes within 150 km of Site 889. With the detection threshold experienced with CORK observatories to date we expect resolvable seismic signals (like those in Fig. F7) several times per year and strain signals (like those in Figs. F6 and F9) once every few years.

Earthquakes within 150 km of Site 889
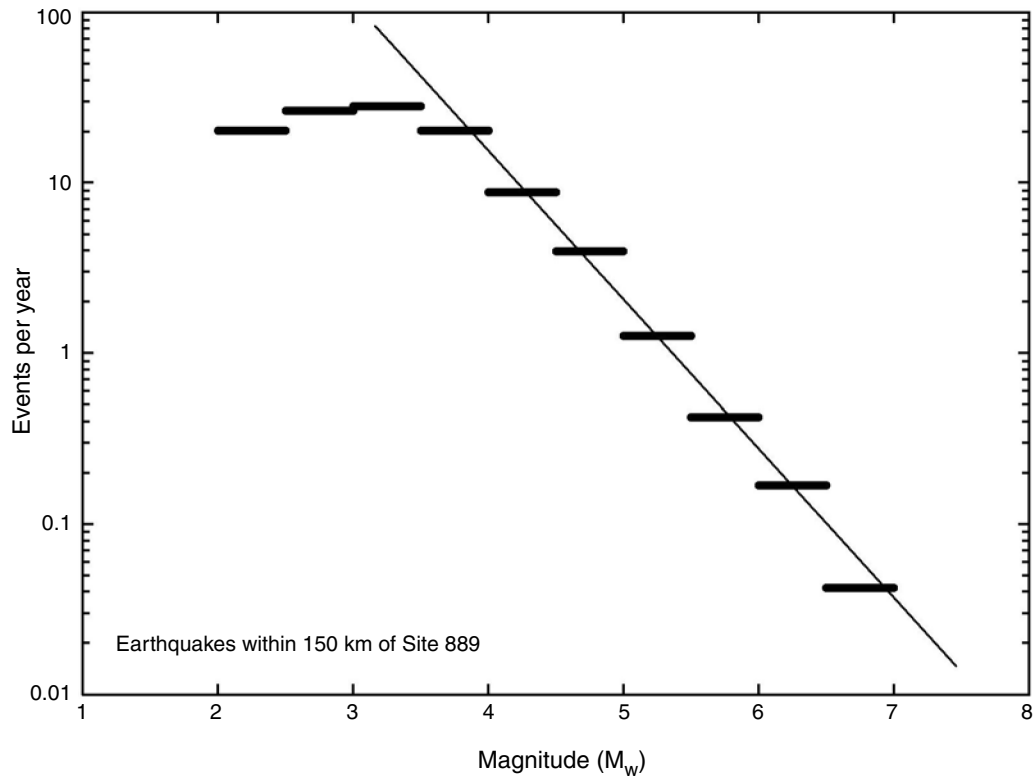
Figure F11. Global Positioning System (GPS) observations (blue circles and fitted saw-tooth function) showing slow eastward displacement above the Cascadia subduction zone and periodic reversals concurrent with increased seismic tremor levels at and above the subduction thrust interface (Fig. F8B). Reversals are caused by slow slip on the subduction plate interface downdip from the currently locked portion of the subduction fault (from Rogers and Dragert, 2003). Slip events like these have been observed to initiate slow rupture that propagates through the seismogenic part of the subduction fault (Heesemann and Davis, submitted).
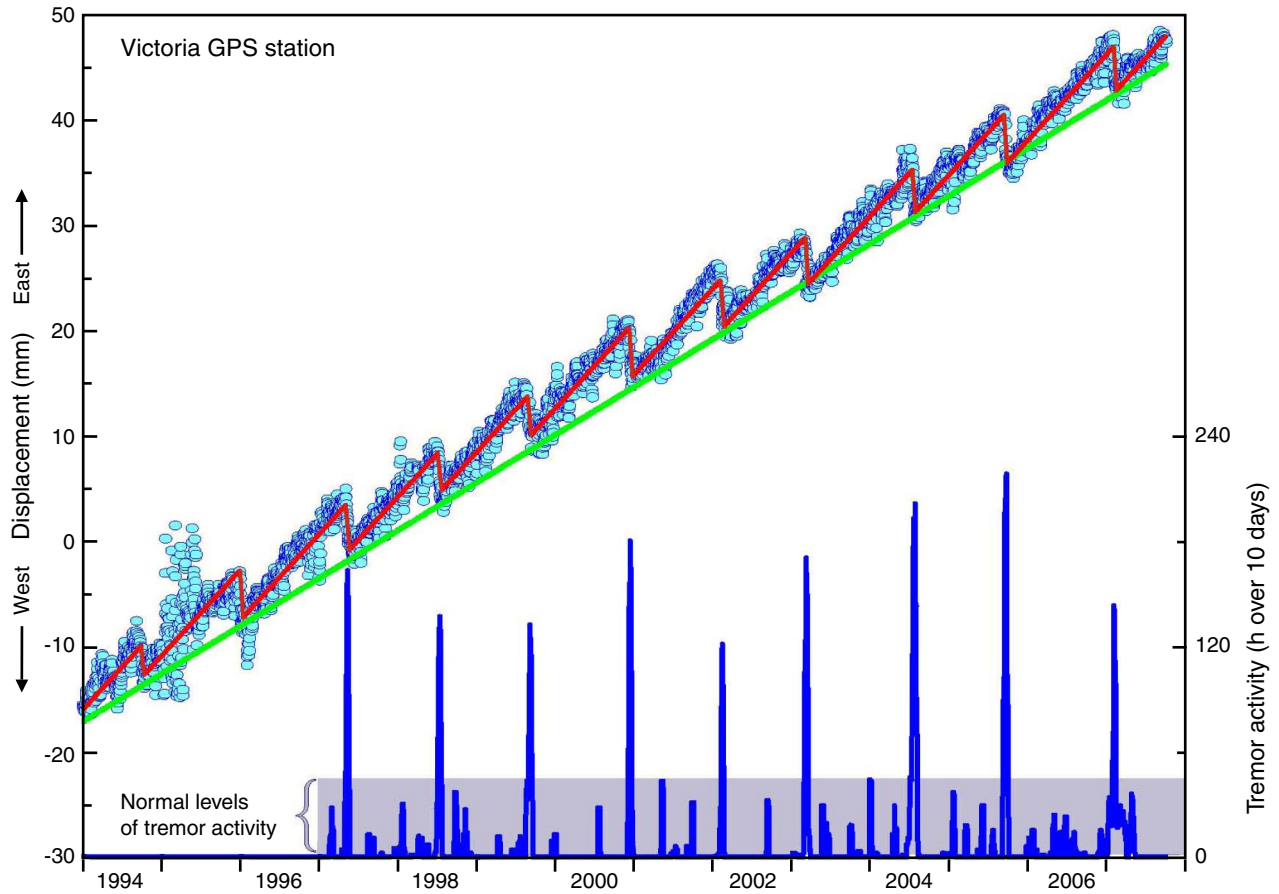
Figure F12. Schematic illustration of ACORK being constructed for deployment during Expedition 328 at Site 889. ROV = remotely operated vehicle, CSG = casing.
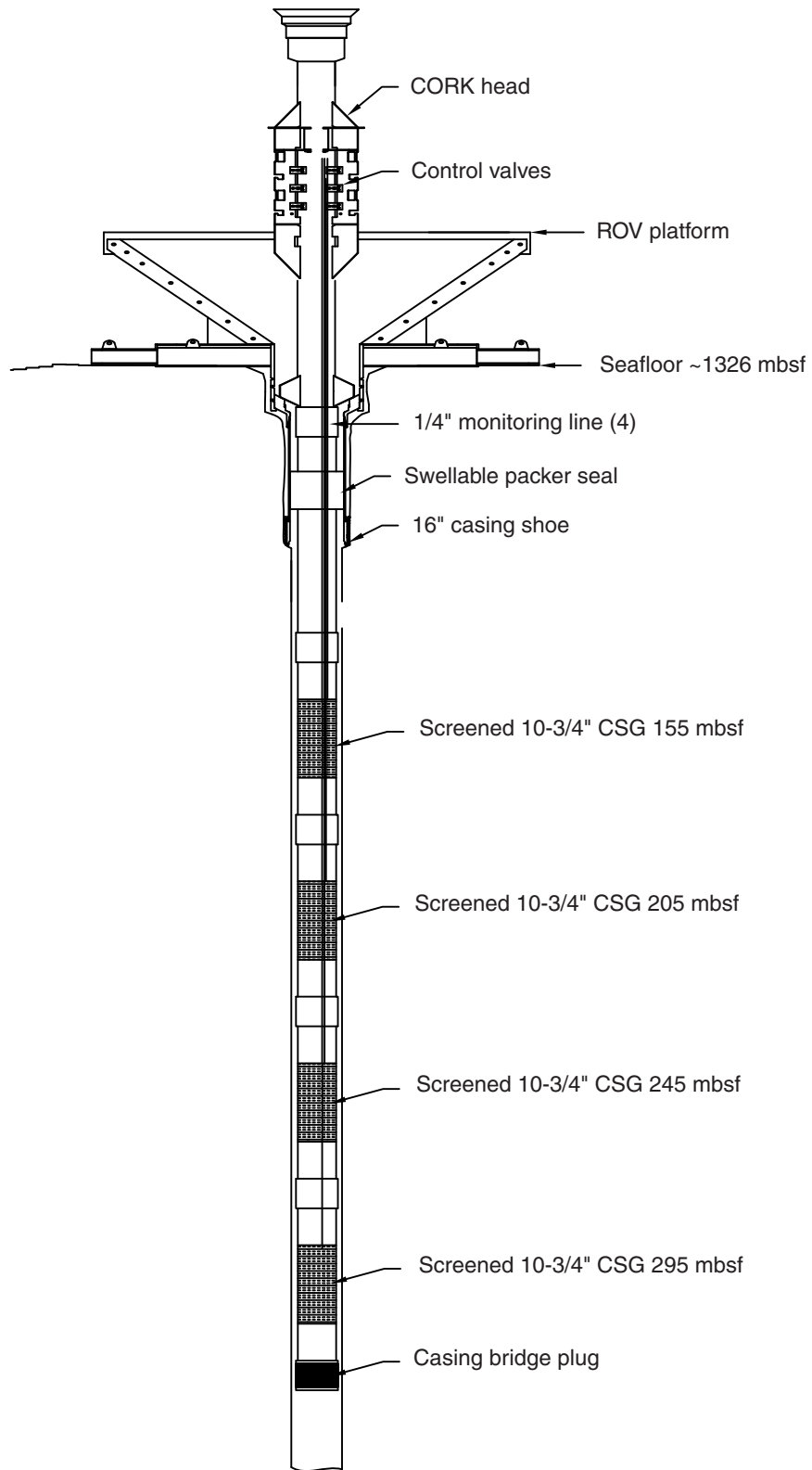
Figure F13. A. Illustration of effects of oceanographic and tectonic loading on formation fluid pressure and flow. **B.** Response to loading can be broken into elastic (instantaneous) and diffusive components. **C.** Transients propagate away from boundaries between regions of contrasting elastic properties as a damped diffusive wave with a characteristic scale that depends on permeability. (**Continued on next page.**)
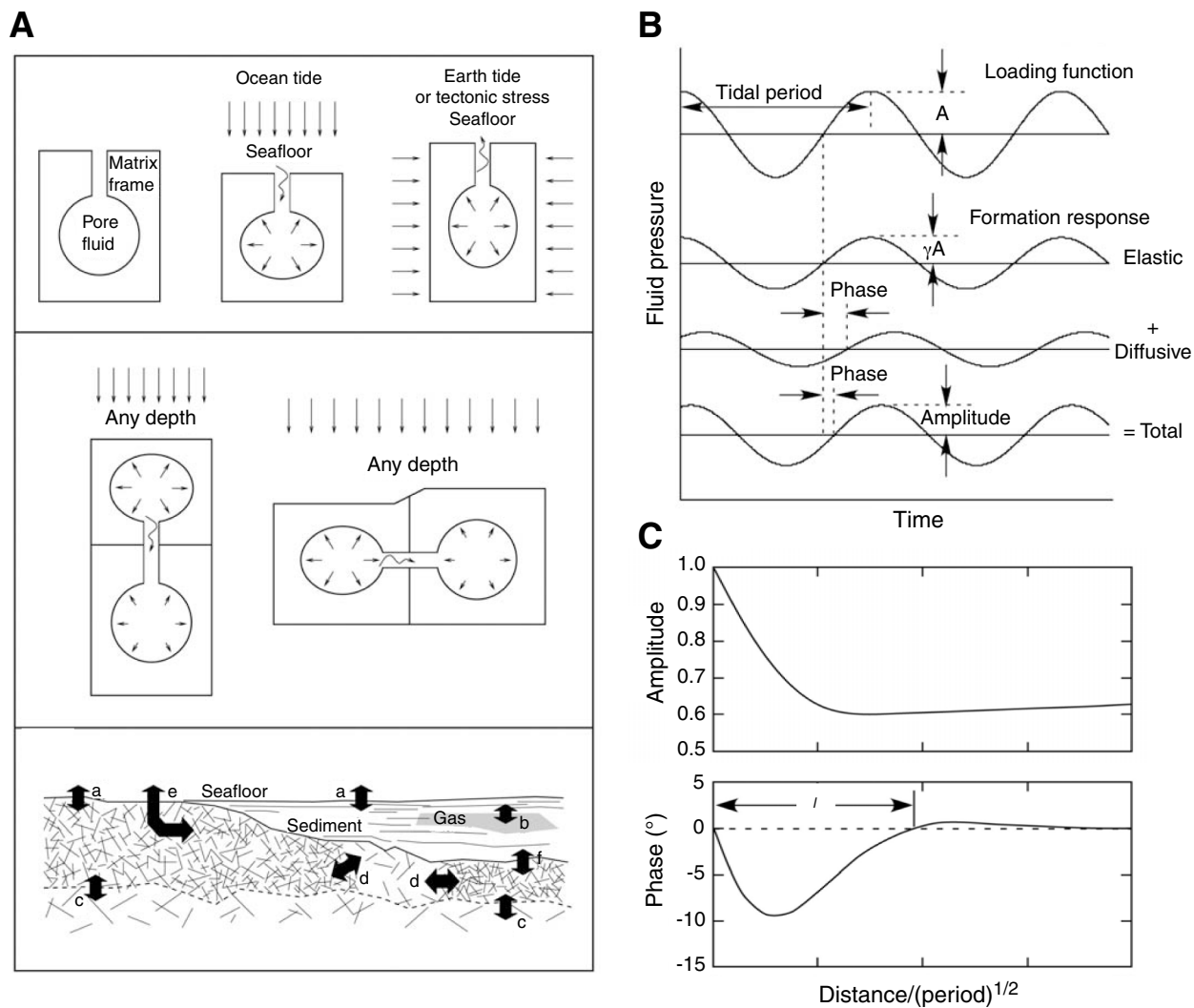
Figure F13 (continued). D. Elastic response expressed as loading efficiency (γ in B) depends on the compressibility of the sediment framework and the compressibility of the interstitial water that may contain free gas. **E.** Response of pressure to volumetric strain in sediment depends primarily on porosity because the compressibility of the matrix is greater than that of water (dotted lines = grain and water compressibilities). (Figures after Wang and Davis, 1996; Wang et al., 1998; and Davis et al., 2000.)
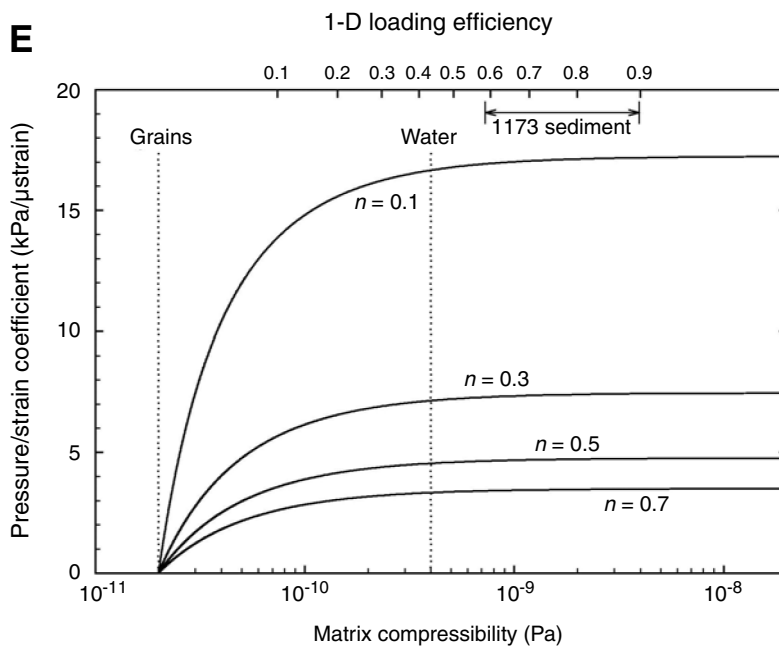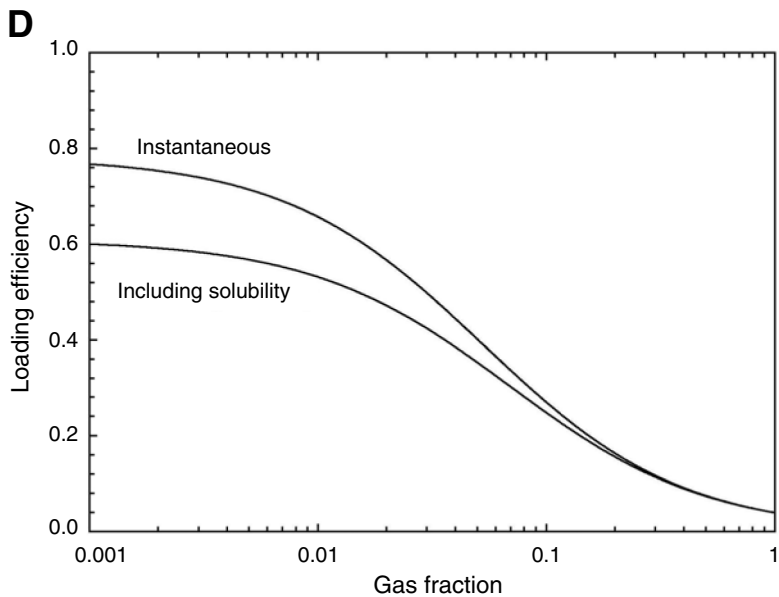
Site summary

Proposed Site CAS-01CORK

Priority:	Primary
Position:	48°41.9964'N, 126°52.3302'W
Water Depth (m):	1315
Target drilling depth (mbsf):	New borehole; penetration ~315 mbsf
Approved maximum penetration (mbsf):	Pending approval
Survey coverage:	Lines 89-08, XL-03 XL-04, IL 33, 35, 37 (Track map Fig. **F1B,** Seismic profiles Fig. **F3**)
Objective (see text for full details):	Install long-term borehole observatory (pressure, tilt, temperature, broadband seismology)
Drilling, coring, and downhole measurement program:	Install new long-term borehole observatory
Anticipated lithology:	Sediment

Scientific participants

The current list of participants for Expedition 328 can be found at **iodp.tamu.edu/scienceops/precruise/cascadia/participants.html.**